JOURNAL OF SOLID STATE CHEMISTRY **140,** 145–148 (1998)
ARTICLE NO. SC987943

LETTER TO THE EDITOR

Study of the Jahn–Teller Distortion in $LiNiO_2$, a Cathode Material in a Rechargeable Lithium Battery, by *in Situ* X-Ray Absorption Fine Structure Analysis

Izumi Nakai,[1] Kouta Takahashi, Youhei Shiraishi, Tatsuji Nakagome, and Fumishige Nishikawa*

*Department of Applied Chemistry, Faculty of Science, Science University of Tokyo, Kagurazaka, Shinjuku, Tokyo 162, Japan; and *Battery Development Laboratory, Asahi Chemical Industry, Ltd., Yako, Kawasaki, Kanagawa 210, Japan*

Communicated by J. W. Richardson June 19, 1997; accepted November 3, 1997

Structural changes accompanying the electrochemical Li deintercalation of $Li_{1-x}NiO_2$ and $Li_{1-x}CoO_2$ were studied by the transmission X-ray absorption fine structure (XAFS) technique using an *in situ* X-ray cell of original design. Our results revealed that the Jahn–Teller distortion of the Ni–O octahedra found in $LiNiO_2$ decreased as the Li ion was removed from the cathode. The observed X-ray absorption near-edge structures (XANES) of $Li_{1-x}NiO_2$ and $Li_{1-x}CoO_2$ as a function of x are consistent with the phase transitions found by powder-diffraction studies. The Ni–O, Co–O, and Ni–Ni interatomic distances decreased almost linearly as the Li content decreased to $x = 0.8$, while the Co–Co distance slightly decreased to $x = 0.5$ and increased up to $x = 0.8$. The local distortion of NiO_6 octahedra also decrease with increasing y in a $Li(Ni_{1-y}, Co_y)O_2$ solid solution.

1. INTRODUCTION

There is a strong demand for long-life rechargeable batteries for use in mobile electronic appliances such as computers and video cameras. $LiCoO_2$ is currently used as the cathode material for secondary lithium batteries because Li can be electrochemically deintercalated to form $Li_{1-x}CoO_2$ (1). There has been an extensive search for electrode materials other than $LiCoO_2$, however, due to the high cost of Co (2–4). $LiNiO_2$ is a promising potential electrode material, although complicated phase transitions in $Li_{1-x}NiO_2$ during the charge–discharge process (5, 6) require a detailed structural characterization.

$LiNiO_2$ is isostructural with $LiCoO_2$, which crystallizes with a rhombohedral layered rock-salt structure (5, 6). Metal ions occupy the octahedral sites of a cubic close-packed network of oxygen ions to form alternate ordered layers of Li and Ni ions parallel to the (111) plane of the cubic rock-salt structure. Rougier *et al.* have reported for the first time the presence of an NiO_6 distortion (two Ni–O bond lengths: four bonds at 1.91 Å and two at 2.09 Å) in $LiNiO_2$ due to the local Jahn–Teller effect of the Ni^{3+} ion based on an XAFS analysis (7). Crystallographically, the Ni atom is located at the 3b site of the $R\bar{3}m$ lattice with six oxygen atoms at equal Ni–O distances. Therefore, the distortion should not occur at long range and cannot be detected by conventional diffraction techniques. XAFS, therefore, is the most suitable technique for examining structural variations in the transition metal atoms during the charge–discharge process. The Li ion is deintercalated from $LiNiO_2$ during the charge process and is intercalated during the discharge process. The present study was conducted to reveal variations in the local structure of the Ni and Co atoms in $Li_{1-x}NiO_2$ and $Li_{1-x}CoO_2$ as a function of Li content by an *in situ* XAFS technique.

2. EXPERIMENTAL

$LiNiO_2$ was prepared by reacting stoichiometric amounts of $LiOH \cdot H_2O$ with $Ni(OH)_2$ at 650°C in air for 3 h. $LiCoO_2$ was obtained by heating Li_2CO_3 and Co_3O_4 in air at 900°C for 3 h. Starting materials of the synthesis of a $LiNi_yCo_{1-y}O_2$ solid solution with various y values were prepared by the coprecipitation method by adding 1 M NaOH solution to a solution of $Ni(NO_3)_2 \cdot 6H_2O$ and $Co(NO_3)_2 \cdot 6H_2O$ in stoichiometric proportions. The precipitate was filtered and dried overnight in an electric drying oven at 120°C. Li_2CO_3 was then added to the precipitate and they were thoroughly mixed with an agate motor. $Li_{1-x}(Ni_{0.5}Co_{0.5})O_2$ was synthesized by heating the mixture in air for 48 h at 750°C. The electrochemical cell used

[1]Author to whom correspondence should be addressed.

0022-4596/98 $25.00

for the *in situ* XAFS measurement was composed of Kapton windows, a cathode material on aluminum foil, a lithium metal anode, and a 1 M electrolyte solution of $LiBF_4$ in propylene carbonate and ethylene carbonate. The Li ion was electrochemically deintercalated from $LiNiO_2$ and $LiCoO_2$ by charging the cell at a constant voltage for 30 min, then keeping it at rest for 1 h. The cell was then placed on the optical bench of a conventional XAFS station (BL-7C, Photon Factory, KEK, Tsukuba, Japan). Samples for non-*in-situ* measurements were prepared by mixing the powder samples with a BN powder to form disks. A Si(111) double-crystal monochromator was used and the intensities of incident and transmitted X-rays were measured by ionization chambers at room temperature. The data were analyzed by conventional methods, including background subtraction using the Victreen function, extraction of EXAFS (extended X-ray absorption fine structure) oscillation $\chi(k)$ by the cubic spline technique, Fourier transform, and Fourier filtering followed by a curve-fitting analysis using REX2 data analysis software (8). A theoretical simulation was performed using FEFF6 (9).

3. RESULTS AND DISCUSSION

The Ni and Co *K*-edge XANES spectra of $Li_{1-x}NiO_2$ and $Li_{1-x}CoO_2$ measured as a function of x are shown in Figs. 1a and 1b, respectively. The Li concentrations (x) were calculated from the known cathode masses and the total charge. From the edge structure it can be seen that as the Li ion is deintercalated, the Ni *K*-edge of $Li_{1-x}NiO_2$ shifts to the higher energy side (Fig. 1a), indicating that Ni^{3+} is oxidized to Ni^{4+}. A steady shift in the spectrum begins when x exceeds 0.13. According to the *in situ* X-ray diffraction analysis (5), the original trigonal H1 phase and the new monoclinic M phase coexist in the region $0.15 < x < 0.25$, which is consistent with the starting point of the edge shift of $Li_{1-x}NiO_2$ (Fig. 1a). On the other hand, the XANES spectrum of $Li_{1-x}CoO_2$ begins to shift when x exceeds 0.15, and a clear change in the spectral shape can be observed at $x = 0.35$ (Fig. 1b). The *in situ* X-ray diffraction analysis of $Li_{1-x}CoO_2$ revealed a first-order transition in the region $0.07 < x < 0.25$ (10) which corresponds to the clear change in shape seen in the XANES spectra. Thus, we found that the spectral changes of $LiNiO_2$ are different from those of $LiCoO_2$ during Li deintercalation. It appears that this deintercalation deforms the electronic structure of the Co atom more significantly than that of the Ni atom. It can be presumed that the Li deintercalation causes a simple variation in the Ni–O distance of the NiO_6 octahedra in the latter phase.

Fourier transforms (FT) of k^3-weighted Ni and Co *K*-edge EXAFS oscillation as a function of x are given in Figs. 2a and 2b, respectively. The FT provides information regarding many coordination shells. The first peak at around 1.5 Å in Fig. 2a corresponds to a Ni–O interaction in the first coordination sphere. The second peak at around 2.4 Å represents a Ni–Ni interaction in the second coordination sphere, with some contribution from the Ni–Li interaction, although this contribution is practically negligible because of the small backscattering amplitude of the Li atom. Similarly, the first and second peaks in Fig. 2b represent Co–O and Co–Co interactions, respectively. A simulated FT pattern was calculated with the FEFF6 code (9) for the $R\bar{3}m$ model (model 1 in Fig. 3) with Li at (0, 0, 0), Ni(Co) at (0, 0, 1/2) and oxygen at (0, 0, 0.241) and this was compared with the calculated patterns for the imaginary monoclinic $C2$ model (10), yielding a distorted NiO_6 octahedron with several (2 + 4) Ni–O distances (models 2–4). The FT pattern for model 1 and that of $LiCoO_2$ in Fig. 2b corresponded reasonably well except for the intensities of the peaks beyond 3 Å. Accordingly, it appears that the peaks at 4.6 and 5.4 Å in Figs. 2 and 3 are mainly due to metal–metal interactions, and a significant focusing effect from multiple scattering can be observed in the latter peak. On the other

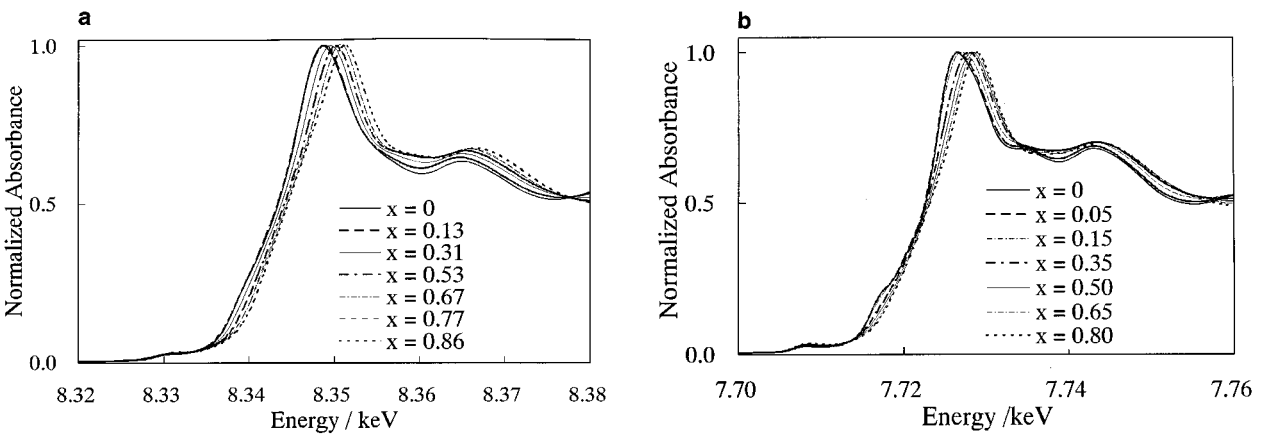

FIG. 1. Ni *K*-edge and Co *K*-edge XANES spectra of (a) $Li_{1-x}NiO_2$ and (b) $Li_{1-x}CoO_2$ as a function of x.

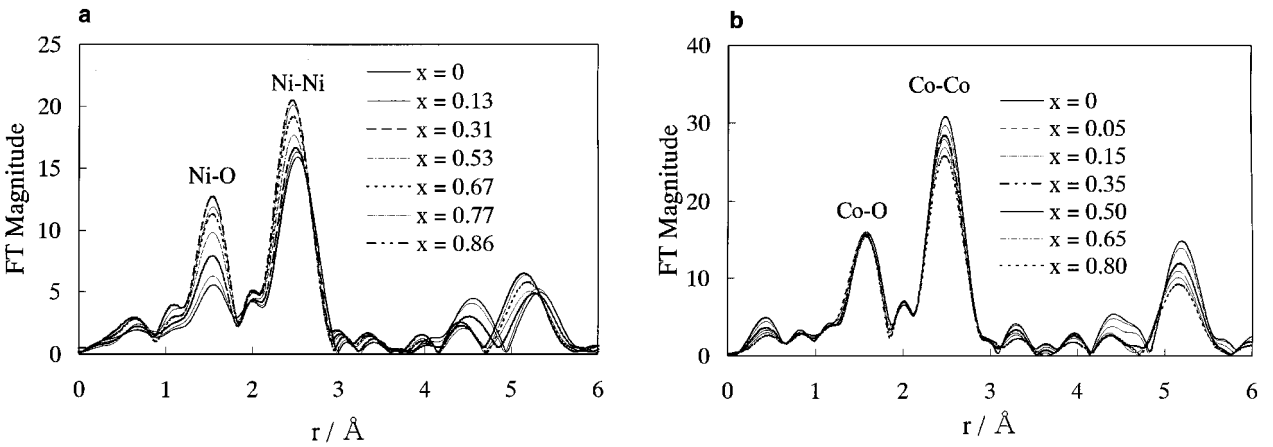

FIG. 2. The Fourier transforms of the Ni *K*-edge and Co *K*-edge EXAFS spectra of (a) $Li_{1-x}NiO_2$ and (b) $Li_{1-x}CoO_2$ as a function of x. The Fourier transforms are not corrected for the phase shifts.

hand, the Ni–O peak for $LiNiO_2$ in Fig. 2a is unexpectedly smaller than Co–O peak in Fig. 2b and the M–O peak for the model 1 (Fig. 3). The small peak for $LiNiO_2$ could be ascribed to the Jahn–Teller distortion from the true octahedral coordination. The distorted (2 + 4) coordination model with 2O at 1.906 and 4O at 2.002 Å (model 3 in Fig. 3) reproduces the experimental FT of $LiNiO_2$ in Fig. 2a, which further supports our interpretation of the small peak for $LiNiO_2$. This apparent decrease in peak height results from the counteractive photoelectron waves produced by X-ray absorption. It is remarkable that the Ni–O peak height increases with the deintercalation of Li, whereas the Co–O peak height remains almost constant (Fig.2). Low-spin Ni^{3+} is the d^7 Jahn–Teller ion with an electronic configuration of $t_{2g}{}^6e_g{}^1$. Deintercalation of Li oxidizes Ni^{3+} to Ni^{4+}, resulting in a $t_{2g}{}^6e_g{}^0$ state with no Jahn–Teller distortion. This is the first observation of a dynamic change in Jahn–Teller effect during the deintercalation process. On the other hand, the oxidation of Co^{3+} causes a removal of the electron from a t_{2g} orbital, not directed at the oxygens and less involved in the metal–metal interaction. Moreover, substituting Co for Ni in $LiNiO_2$ causes an increase in the Ni–O peak heights (Fig 4). This phenomenon can also be explained by the Jahn–Teller effect, with the substitution of $Co^{3+}(d^6)$ for $Ni^{3+}(d^7)$ possibly reducing the local distortion of the Ni octahedra. The existence of a Jahn–Teller effect in $LiNiO_2$ may account for the instability of $LiNiO_2$ as a cathode material. It has been reported that partially substituting Co for Ni improves the quality of a battery (11). The present study has revealed that this Co substitution reduces the Jahn–Teller effect.

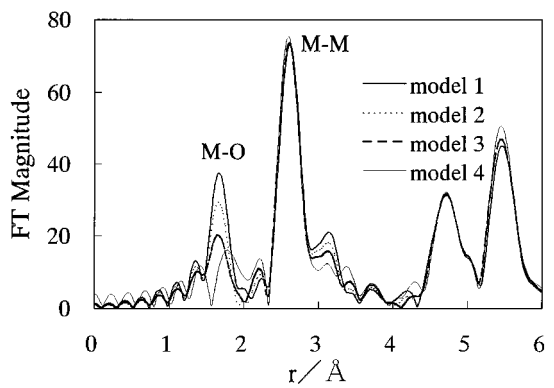

FIG. 3. Simulated Fourier transforms for LiMO_2 (M = Ni, Co). The difference between $LiNiO_2$ and $LiCoO_2$ is practically negligible in the results. Model 1: *R*3*m* (space group) model with regular M–O_6 octahedra with 6O at equal distance; Model 2: *C*2 (space group) model with distorted octahedra with 2O at 1.927 and 4O at 1.991; Model 3: 2O at 1.906 and 4O at 2.002; Model 4: 2O at 1.865 and 4O at 2.025 Å.

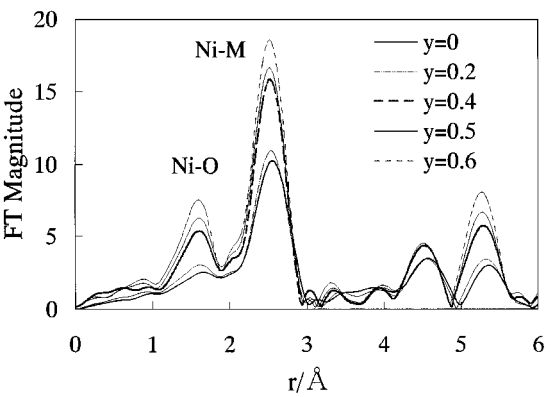

FIG. 4. The Fourier transforms of the Ni *K*-edge EXAFS spectra of $Li(Ni_{1-y}Co_y)O_2$ solid solutions as a function of y. The Fourier transforms are not corrected for the phase shifts.

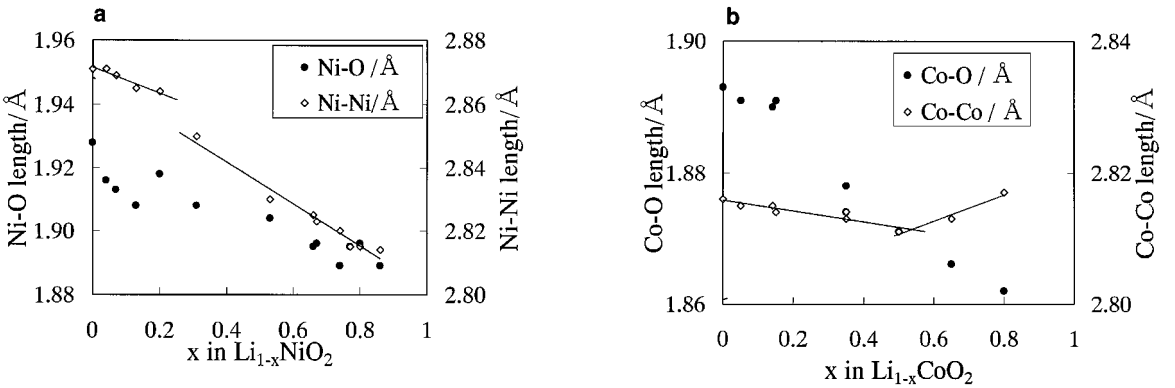

FIG. 5. The metal–oxygen and metal–metal distance as a function of x obtained from the EXAFS analysis of (a) $Li_{1-x}NiO_2$ and (b) $Li_{1-x}CoO_2$, assuming a single metal–oxygen distance and a single metal–metal distance with a coordination number of 6. The linear lines were calculated for the metal–metal distances by the least-squares fitting method.

The metal–oxygen and metal–metal distances were analyzed by Fourier filtering and a curve-fitting analysis of the first and second shells in the FT (Fig. 2). The average Ni–O (Co–O) distance was calculated by assuming a single metal–oxygen shell with coordination number 6, and the Ni–Ni (Co–Co) distance was calculated by assuming a single metal–metal distance with coordination number 6. These results are plotted as a function of x in Figs. 5a and 5b. Both the Ni–O and Co–O bond distances exhibit a linear decrease with a decrease in the Li content. The increase in the average positive charge of the metal atoms with Li deintercalation accounts for the shortening of the metal–oxygen distance. It is noteworthy that the Ni–Ni distance decreased as much as 0.06 Å with x, whereas the decrease in the Co–Co distance was less significant, and the distance actually increased from $x = 0.5$ to $x = 0.8$. These metal–metal distances correspond to the a lattice parameter of the trigonal $R3m$ cell. It is found that the plots of the Ni–Ni distances vs x can be fitted with two straight lines by least-squares methods with a clear discontinuity at around $x = 0.25$ (Fig. 5a). The *in situ* diffraction analysis of $LiNiO_2$ disclosed a trigonal- (hexagonal-) to monoclinic transition at around 0.25, and a variation of the lattice parameters similar to Fig. 5a was reported (5). Similarly, the V shape variation of the Co–Co distances in Fig. 5b is consistent with that determined by the *in situ* diffraction analysis of $LiCoO_2$ (12). The present results, including the XANES features, indicate the consistency between our *in situ* XAFS data and the diffraction data. Further analysis of the XAFS data including quantitative evaluation of the Jahn–Teller distortion of the metal–oxygen octahedra, which could not be revealed by the diffraction technique, is now in progress.

ACKNOWLEDGMENTS

The authors are grateful to Mr. T. Himeda for his kind help in the electrochemical experiments. They thank Mr. T. Konishi for supporting this work. The XAFS experiments were performed under the approval of the PF program Advisory Committee (96G181).

REFERENCES

1. K. Mizushima, P. C. Jones, P. J. Wiseman, and J. B. Goodenough, *Mater. Res. Bull.* **15,** 783 (1980).
2. K. Brandt, *Solid State Ionics* **69,** 173 (1994).
3. J. B. Goodenough, *Solid State Ionics* **69,** 184 (1994).
4. T. Ohzuku and A. Ueda, *Solid State Ionics* **69,** 201 (1994).
5. W. Li, J. N. Reimers, and J. R. Dahn, *Solid State Ionics* **67,** 123 (1993).
6. R. Kanno, H. Kubo, Y. Kawamoto, T. Kamiyama, F. Izumi, and M. Takano, *J. Solid State Chem.* **110,** 216 (1994).
7. A. Rougier, C. Delmas, and A. V. Chadwick, *Solid State Commun.* **94,** 123 (1995).
8. Rigaku, "EXAFS analysis software," REX2, Cat. No. 2612S211. Rigaku Co., 1996.
9. S. I. Zabinsky, J. J. Rehr, A. Ankudinov, R. C. Albers, and M. J. Eller, *Phys. Rev. B* **52,** 2995 (1995).
10. J. N. Reimers and J. R. Dahn, *J. Electrochem. Soc.* **139,** 2091 (1992).
11. T. Nishisawa, Y. Yamamoto, H. Kato, and Y. Nishi, *in* "The 63rd Annual Conference of the Electrochemical Society of Japan," Abstract No. 3D03, p. 107. Tokyo, 1996.
12. G. G. Amatucci, J. M. Tarascon, and L. C. Klein, *J. Electrochem. Soc.* **143,** 1114 (1996).
13. I. Nakai, K. Takahashi, Y. Shiraishi, T. Nakagome, F. Izumi, Y. Ishii, F. Nishikawa, and T. Konishi, *J. Power Sources* **68,** 536 (1997). [Proceedings of 8th Int. Meetings on Lithium Batteries, Nagoya, June 16–21, 1996]